

Synthesis and thermal analysis of indium-based hydrotalcites of formula $Mg_6In_2(CO_3)(OH)_{16}\cdot4H_2O$

Ray L. Frost · Sara J. Palmer · Laure-Marie Grand

Received: 5 August 2009 / Accepted: 18 August 2009 / Published online: 10 September 2009
© Akadémiai Kiadó, Budapest, Hungary 2009

Abstract Insight into the unique structure of layered double hydroxides (LDHs) has been obtained using a combination of X-ray diffraction and thermal analysis. Indium containing hydrotalcites of formula $Mg_4In_2(CO_3)(OH)_{12}\cdot4H_2O$ (2:1 In-LDH) through to $Mg_8In_2(CO_3)(OH)_{18}\cdot4H_2O$ (4:1 In-LDH) with variation in the Mg:In ratio have been successfully synthesised. The $d(003)$ spacing varied from 7.83 Å for the 2:1 LDH to 8.15 Å for the 3:1 indium containing LDH. Distinct mass loss steps attributed to dehydration, dehydroxylation and decarbonation are observed for the indium containing hydrotalcite. Dehydration occurs over the temperature range ambient to 205 °C. Dehydroxylation takes place in a series of steps over the 238–277 °C temperature range. Decarbonation occurs between 763 and 795 °C. The dehydroxylation and decarbonation steps depend upon the Mg:In ratio. The formation of indium containing hydrotalcites and their thermal activation provides a method for the synthesis of indium oxide-based catalysts.

Keywords Hydrotalcite synthesis · Hydrocalumite · Raman spectroscopy · Indium

Introduction

The quest for developing new materials for catalytic purposes is on-going [1–5]. One methodology is to use thermally transformed hydrotalcites or layered double hydroxides (LDHs) as a source of catalyst materials [6–8]. The advantage of using thermally activated hydrotalcites is that mixed oxides are formed which are mixed at the atomic level and not at the particle level. Thus, this methodology offers a high surface area suitable for catalysts [4, 9–11]. Indium oxides mixed with other oxides have potential catalytic properties. Whilst there have been several studies of LDHs containing gallium [12–15], there have been very few studies of LDHs containing indium [1, 2, 16, 17]. Further methodical studies of LDHs based upon indium as the trivalent cation have not been forthcoming.

Hydrotalcites or LDHs, have been known for an extended period of time [18–20]. Hydrotalcites are fundamentally known as anionic clays [21]. Hydrotalcites consist of stacked layers of metal cations (M^{2+} and M^{3+}) similar to brucite ($Mg(OH)_2$). The structure of hydrotalcite can be derived from a brucite structure ($Mg(OH)_2$) in which, e.g. Al^{3+} or Fe^{3+} (pyroaurite–sjögrenite) substitutes a part of the Mg^{2+} [19, 22–24]. The trivalent cation is not restricted to these cations but may also be based upon In^{3+} . Any trivalent cation may substitute for aluminium in the brucite layer. The ionic radii of Mg^{2+} , Al^{3+} and In^{3+} are 0.066, 0.056 and 0.081 nm. This substitution creates a positive layer charge on the hydroxide layers, which is compensated by anions held within the interlayer. In general, any trivalent cation may substitute for the Al^{3+} in the brucite-like layer. Hydrotalcites consist of stacked layers of metal cations (M^{2+} and M^{3+}) similar to brucite ($Mg(OH)_2$). For hydrotalcite-like structures, the substitution of divalent cations for trivalent ones (of similar radii), gives rise to a

R. L. Frost (✉) · S. J. Palmer · L.-M. Grand
Inorganic Materials Research Program, School of Physical
and Chemical Sciences, Queensland University of Technology,
GPO Box 2434, Brisbane, QLD 4001, Australia
e-mail: r.frost@qut.edu.au

L.-M. Grand
ENSICAEN, 6 Boulevard Marechal Juin, 14050 Caen Cedex 4,
France

positive charge on the brucite-like layers. In hydrotalcites a broad range of compositions are possible of the type $[M_{1-x}^{2+}M_x^{3+}(OH)_2]_{x/n} \cdot yH_2O$, where M^{2+} and M^{3+} are the di- and trivalent cations in the octahedral positions within the hydroxide layers with x normally between 0.17 and 0.33. A''^- is an exchangeable interlayer anion [25]. The positively charged hydroxyl layers are neutralised through the intercalation and adsorption of anionic species, therefore stabilising the structure. Anions that are intercalated between the hydroxyl layers need to meet certain criteria, including having a high charge density and small anionic radius.

Recent studies have proven the usefulness of thermoanalytical techniques for the study of the thermal stability of minerals and compounds of interest in catalysis [26–39]. Very few studies of the replacement of the aluminium by indium have been reported [1, 2, 16, 17]. There is some evidence that in bauxite, indium is found as a very low level impurity as indium trihydroxide [27, 40, 41]. The reaction of red mud and sea water results in the formation of hydrotalcites based not only upon aluminium but also trivalent cations including indium. This is the basis for the underlying reason why this research is being undertaken. This study focusses upon the synthesis and thermoanalytical characterisation of hydrotalcites with indium substituting for aluminium in the brucite layer.

Experimental

Synthesis of hydrotalcite samples

Hydrotalcites can be synthesised in the laboratory using analytical grade chemicals. The reason for using synthetic compounds as opposed to the natural minerals are that difficulties associated with multiple anions in the interlayer can be minimised, and allow for trends and characteristics to be more readily determined. In this case a range of Mg–In with varying ratios has been synthesised.

The hydrotalcites were synthesised by the co-precipitation method. The amounts and concentrations of the ingredients used for the synthesis of the indium containing hydrotalcites are provided in Table 1. Two solutions were

Table 1 Table of concentrations of chemicals used in the synthesis of indium containing hydrotalcites

	2:1	2.5:1	3:1	3.5:1	4:1
Concentration of $MgCl_2 \cdot 6H_2O/M$	0.67	0.71	0.75	0.77	0.80
Masses of $MgCl_2 \cdot 6H_2O/g$	3.40	3.63	3.81	3.96	4.07
Concentration of $InCl_3/M$	0.33	0.29	0.25	0.22	0.20
Masses of $InCl_3/g$	1.82	1.58	1.38	1.23	1.11

prepared, solution 1 contained 2 M NaOH and 0.2 M Na_2CO_3 , and solution 2 contained Mg^{2+} ($MgCl_2 \cdot 6H_2O$) at different concentrations, together with $InCl_3$. Solution 2 was added at a steady rate to solution 1 drop wise, under vigorous stirring. A separating funnel was used to deliver solution 2 to solution 1. The precipitated minerals were washed at ambient temperatures thoroughly with ultra pure water to remove any residual salts and dried in an oven ($\lesssim 85$ °C) overnight.

X-ray diffraction

X-ray diffraction patterns were collected using a Philips X'pert wide angle X-Ray diffractometer, operating in step scan mode, with $Cu K\alpha$ radiation (1.54052 Å).

Thermal analysis

Thermal decomposition of approximately 50 mg of hydrotalcite was carried out in a TA® Instruments incorporated high-resolution thermogravimetric analyser (series Q500) in a flowing nitrogen atmosphere (80 cm³/min), at a rate of 2.0 °C/min up to 1000 °C. For more information on the experimental and analysis techniques used, refer to previous work by the authors [26, 27, 30, 35–37].

Results and discussion

X-ray diffraction

Hydrotalcites both synthetic and natural are normally in the first instance characterised, by X-ray diffraction in order to confirm their layered structures. This enables proof of the structure of the layered material to be obtained. A typical pattern will show the $d(003)$ peak and consequential diffraction peaks. The powder XRD patterns of the synthesised magnesium–indium containing LDHs are shown in Fig. 1 together with possible impurity phases. Possible impurities include sodium chloride and dzhalindite ($In(OH)_3$). The synthesised indium containing LDHs show excellent purity. The width of the $d(003)$ peaks provided evidence that the indium based hydrotalcites are highly crystalline.

The $d(003)$ spacing for a series of magnesium–indium containing LDHs with varying Mg/In ratios varies from 7.78 Å for the 2:1 LDHs to 8.09 Å for the 3.5:1 indium containing LDHs. The $d(003)$ spacing for a typical Mg/Al hydrotalcite varies from 7.62 Å for the 2:1 Mg hydrotalcite to 7.98 Å for the 4:1 hydrotalcite. The interlayer spacing for the hydrotalcite based upon Mg/In is higher than that for the Mg/Al hydrotalcite. This difference in the interlayer spacing is accounted for by the size of the In^{3+} cation. The ionic radii of Mg^{2+} and In^{3+} are 0.066 and 0.081 nm. Li

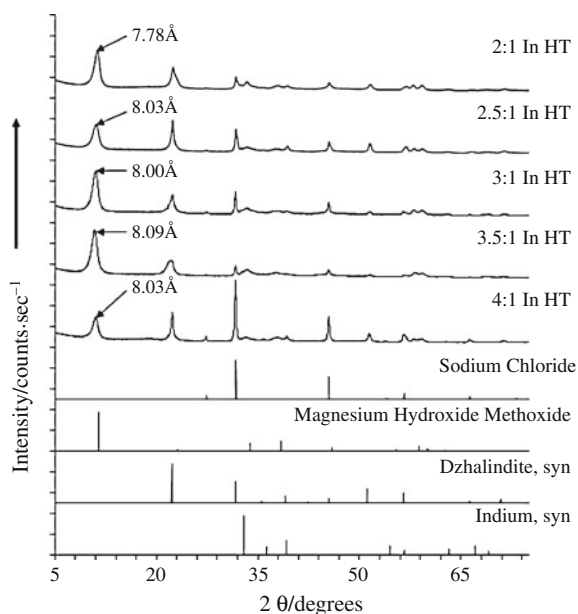


Fig. 1 XRD patterns of indium-based hydrotalcites with Mg:In varying from 2:1 to 4:1 together with reference patterns

et al. [3] reported the unit cell dimensions of a 3:1 Mg:In LDH and compared the a and c parameters for 3:1 Mg:Al and Mg/Al/In LDHs.

Thermal analysis

The thermal analysis of the 3:1 $Mg_6In_2(CO_3)(OH)_{16}\cdot 4H_2O$ and 2:1 $Mg_4In_2(CO_3)(OH)_{12}\cdot 4H_2O$ indium containing hydrotalcites are reported in Figs. 2 and 3. A comparison of the thermal analysis patterns of the 2:1, 3:1 and 4:1 indium containing hydrotalcites is displayed in Fig. 4. A number of mass loss steps are observed for the 3:1 In HT (Fig. 2). The first mass loss of 2.44% occurs at low temperatures below 50 °C. This mass loss is attributed to the loss of adsorbed water. A further mass loss of 8.44% assigned to the loss of structural water contained within the HT interlayer is observed over the 60–209 °C temperature range. Based upon

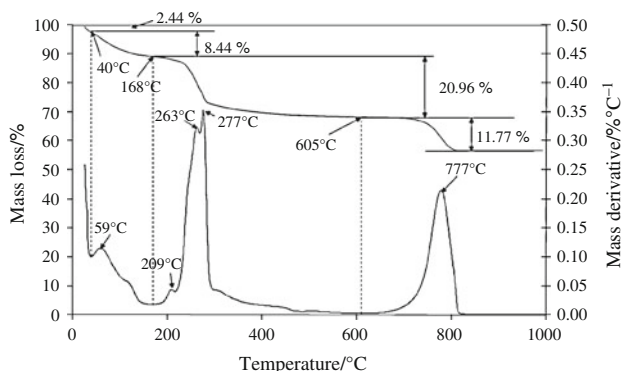


Fig. 2 Thermogravimetry of 3:1 indium hydrotalcite

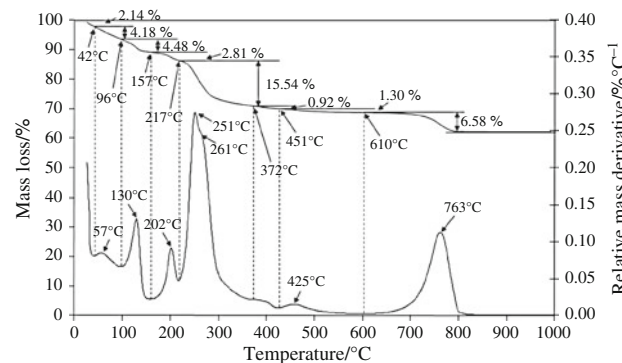


Fig. 3 Thermogravimetry of 2:1 indium hydrotalcite

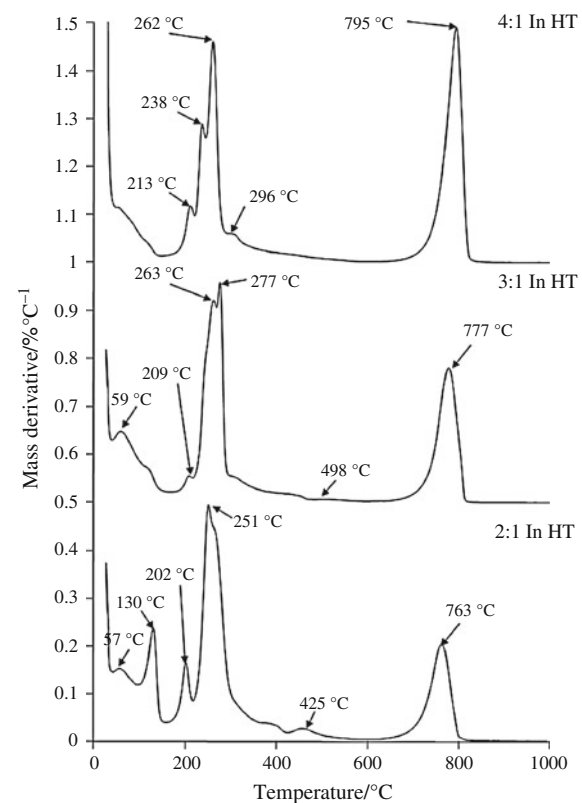


Fig. 4 Derivative thermogravimetry of 2:1, 3:1 and 4:1 indium hydrotalcite

the formula of the 3:1 HT $\text{Mg}_6\text{In}_2(\text{CO}_3)_9(\text{OH})_{16} \cdot 4\text{H}_2\text{O}$, the theoretical mass loss of structural water is 9.28% which compares well with the experimental result of 8.44%.

Three mass loss steps are observed at 209, 263 and 277 °C. The total mass loss over these three decomposition steps was calculated as 20.96%. Ion current mass spectrometry indicates water is lost over the 200–300 °C temperature range. The theoretical mass loss due to dehydroxylation is 18.55% which is in harmony with the experimentally determined result. A higher temperature mass loss step is observed at 777 °C with a mass loss of 11.77%. This mass loss step is ascribed to the loss of

carbon dioxide. The theoretical mass loss of CO₂ is 7.73%. The experimental value is larger than the theoretical number.

The 2:1 In HT thermal analysis patterns are reported in Fig. 3. There is a strong resemblance between the thermal analysis patterns of the 2:1 In HT with the 3:1 In HT. Distinct mass loss steps are observed at 57, 130, 202, 251 and 763 °C. The low temperature mass loss of 2.14% is attributed to the desorption of surface water. Two mass loss steps of 4.18 and 4.48% are observed at 59 and 130 °C. These mass loss steps are ascribed to the loss of interlayer water held between the hydrotalcite layers. The three mass loss steps at 202, 251 and 261 °C are assigned to dehydroxylation. Ion current mass spectrometry indicates some carbon dioxide is lost at these temperatures as well. It is understood that most of the carbonate is retained and is lost at the higher temperature of 763 °C.

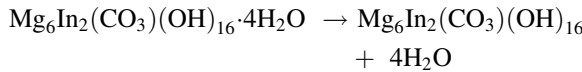
A comparison of the thermal decomposition of the 4:1, 3:1 and 2:1 indium containing hydrotalcites is shown in Fig. 4. Subtle changes are occurring as the ratio of Mg:In is changed from 2:1 to 4:1. The temperature of the mass loss step assigned to decarbonation shifts from 763 °C for the 2:1 In HT to 777 °C for the 3:1 In HT to 795 °C for the 4:1 In HT. The two overlapping mass loss steps at 251 and 261 °C show greater separation as the ratio of the Mg:In changes from 2:1 through 3:1 to 4:1. These mass loss peaks change from 251 and 261 °C for the 2:1 In HT, to 263 and 277 °C for the 3:1 In HT, to 262 and 238 °C for the 4:1 In HT. Also there appears to be less water associated with the 4:1 In HT compared with the 2:1 In HT.

Mechanism for the decomposition of indium-based hydrotalcites

Based upon the 3:1 In HT Mg₆In₂(CO₃)(OH)₁₆·4H₂O, the following steps are proposed:

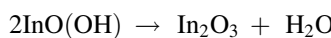
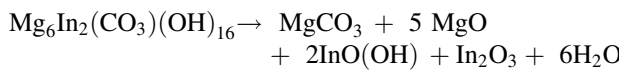
Step 1 dehydration

Temperature range ambient up to 205 °C



Step 2 dehydroxylation

Temperature range 210 to 280 °C. A two-step process is envisaged.



Step 2 decarbonation



Conclusions

Indium containing hydrotalcites of formula Mg₄In₂(CO₃)(OH)₁₂·4H₂O (2:1 In-LDH) to Mg₈In₂(CO₃)(OH)₁₈·4H₂O (4:1 In-LDH) have been successfully synthesised and characterised by X-ray diffraction and thermoanalytical techniques. The XRD patterns proved that the In-LDHs were synthesised with high purity. Indium containing hydrotalcites of formula Mg₄In₂(CO₃)(OH)₁₂·4H₂O (2:1 In-LDH) through to Mg₈In₂(CO₃)(OH)₁₈·4H₂O (4:1 In-LDH) with variation in the Mg:In ratio have been successfully synthesised. The *d*(003) spacing varied from 7.83 Å for the 2:1 LDH to 8.15 Å for the 3:1 indium containing LDH.

Distinct mass loss steps attributed to dehydration, dehydroxylation and decarbonation are observed for the indium containing hydrotalcite. Dehydration occurs over the temperature range ambient to 205 °C. Dehydroxylation takes place in a series of steps over the 238–277 °C temperature range. Decarbonation occurs between 763 and 795 °C. The dehydroxylation and decarbonation steps depend upon the Mg:In ratio. The formation of indium containing hydrotalcites and their thermal activation provides a method for the synthesis of indium oxide-based catalysts.

Acknowledgements The financial and infra-structure support of the Queensland Research and Development Centre (QRDC-RioTintoAlcan) and the Queensland University of Technology Inorganic Materials Research Program of the School of Physical and Chemical Sciences are gratefully acknowledged. The Australian Research Council (ARC) is thanked for funding the instrumentation.

References

- Choudhary VR, Jha R, Narkhede VS. In-Mg-hydrotalcite anionic clay as catalyst or catalyst precursor for Friedel-Crafts type benzylation reactions. *J Mol Catal A*. 2005;239:76–81.
- Gabrovska M, Edreva-Kardjieva R, Angelov V, Crisan D, Munteanu G, Vedrine J. Mg-Al and Mg-In oxide compounds as catalyst components for the oxidative dehydrogenation of propane. Part I. Preparation and characterization of the as-synthesized materials. *Revue Roumaine de Chimie*. 2007;52:521–5.
- Li F, Jiang X, Evans DG, Duan X. Structure and basicity of mesoporous materials from Mg/Al/In layered double hydroxides prepared by separate nucleation and aging steps method. *J Porous Mater*. 2005;12:55–63.
- Xiang X, Wang H, Li F. Layered double hydroxides/carbon nanotube heterostructure material and its preparation by L-cysteine based assembly of layered double hydroxides. Beijing University of Chemical Technology, People's Republic of China, Application, CN CN; 2007, 10 pp.
- Yang W, Wang Y, Zhang X. Method for preparing MnO₂/hydrotalcite inorganic nanosheet composite ultrathin film. Beijing University of Chemical Technology, People's Republic of China, Application, CN CN; 2007, 16 pp.
- Okada K, Mimura K, Nogi S. Synthesis of hydrotalcite-type layered compounds, M(II)_{1-x}In_x(OH)₂(NO₃)_x·nH₂O (M = Ni, Mg, Co, and Ca). *Nendo Kagaku*. 1994;34:40–7.

7. Swamy CS, Kannan S, Li Y, Armor JN, Braymer TA. Method for decomposing N2O utilizing catalysts comprising calcined anionic clay minerals. Air Products and Chemicals, Inc., USA, Application, EP EP; 1995, 19 pp.
8. Wang P, Li M, Chen H, Zhang W, Da Z, Tian H, Luo Y, Zong B, He M, Long J. Manufacture of cracking catalyst for hydrocarbon with desulfurization function. (China Petroleum and Chemical Corporation, People's Republic of China, Research Institute of Petroleum Processing, China Petroleum and Chemical Corporation, Application, CN CN; 2005, 25 pp.
9. Duan X, Li F, Zou L. Method for manufacturing spinel nanoparticles with high specific surface area from lamellar precursor. Beijing University of Chemical Technology, People's Republic of China, Application, CN CN; 2005, 6 pp.
10. Prihod'ko R, Sychev M, Kolomitsyn I, Stobbelaar PJ, Hensen EJM, van Santen RA. Layered double hydroxides as catalysts for aromatic nitrile hydrolysis. *Microporous Mesoporous Mater.* 2002; 56:241–55.
11. Weir MR, Kydd RA. Synthesis of heteropolyoxometalate-pillared Mg/Al, Mg/Ga, and Zn/Al layered double hydroxides via LDH-hydroxide precursors. *Inorg Chem.* 1998;37:5619–24.
12. Altuntasoglu O, Unal U, Ida S, Goto M, Matsumoto Y. Characterization of self-assembled films of NiGa layered double hydroxide nanosheets and their electrochemical properties. *J Solid State Chem.* 2008;181:3257–63.
13. Aramendia MA, Borau V, Jimenez C, Marinas JM, Romero FJ, Ruiz JR. Synthesis, characterization, and 1H and 71 Ga MAS NMR spectroscopy of a novel Mg/Ga double layered hydroxide. *J Solid State Chem.* 1997;131:78–83.
14. Defontaine G, Michot LJ, Bihannic I, Ghanbaja J, Briois V. Synthesis of NiGa layered double hydroxides. A combined EXAFS, SAXS, and TEM study. 2. Hydrolysis of a Ni²⁺/Ga³⁺ solution. *Langmuir.* 2004;20:9834–43.
15. Fuda K, Kudo N, Kawai S, Matsunaga T. Preparation of zinc/gallium-layered double hydroxide and its thermal decomposition behavior. *Chem Lett.* 1993; 5:777–80.
16. Aramendia MA, Borau V, Jimenez C, Marinas JM, Luque JM, Ruiz JR, et al. Synthesis and characterization of a novel Mg/In hydrotalcite-like compound. *Mater Lett.* 2000;43:118–21.
17. Liu P, Zheng J-h, Pi Z-b, Qiao X-h. Synthesis and characterization of magnesium–aluminum–indium hydrotalcite-like compounds. *Diqu Kexue.* 2003;28:163–6.
18. Allmann R. Crystal structure of pyroaurite. *Acta Cryst.* 1968; B24:972–7.
19. Ingram L, Taylor HFW. Crystal structures of sjogrenite and pyroaurite. *Mineral Mag.* 1967;36:465–79.
20. Taylor HFW. Crystal structures of some double hydroxide minerals. *Mineral Mag.* 1973;39:377–89.
21. Rives V, editor. Layered double hydroxides: present and future. New York: Nova Science Publisher Inc.; 2001.
22. Brown G, Van Oosterwyck-Gastuche MC. Mixed magnesium-aluminum hydroxides. II. Structure and structural chemistry of synthetic hydroxycarbonates and related minerals and compounds. *Clay Miner.* 1967;7:193–201.
23. Taylor HFW. Segregation and cation-ordering in sjogrenite and pyroaurite. *Mineral Mag.* 1969;37:338–42.
24. Taylor RM. Stabilization of color and structure in the pyroaurite-type compounds iron(II) iron(III) aluminum(III) hydroxycarbonates. *Clay Miner.* 1982;17:369–72.
25. Kloprogge JT, Wharton D, Hickey L, Frost RL. Infrared and Raman study of interlayer anions CO₃²⁻, NO⁻³, SO₄²⁻ and ClO⁻⁴ in Mg/Al-hydrotalcite. *Am Miner.* 2002;87:623–9.
26. Frost RL, Hales MC, Martens WN. Thermogravimetric analysis of selected group (II) carbonate minerals—implication for the geosequestration of greenhouse gases. *J Therm Anal Calorim.* 2009; 95:999–1005.
27. Palmer SJ, Spratt HJ, Frost RL. Thermal decomposition of hydrotalcites with variable cationic ratios. *J Therm Anal Calorim.* 2009;95:123–9.
28. Carmody O, Frost R, Xi Y, Kokot S. Selected adsorbent materials for oil-spill cleanup. A thermoanalytical study. *J Therm Anal Calorim.* 2008;91:809–16.
29. Frost RL, Locke AJ, Martens WN. Thermogravimetric analysis of wheatleyite Na₂Cu²⁺(C₂O₄)₂·2H₂O. *J Therm Anal Calorim.* 2008; 93:993–7.
30. Frost RL, Locke AJ, Hales MC, Martens WN. Thermal stability of synthetic aurichalcite. Implications for making mixed metal oxides for use as catalysts. *J Therm Anal Calorim.* 2008;94:203–8.
31. Frost RL, Locke AJ, Martens W. Thermal analysis of beaverite in comparison with plumbojarosite. *J Therm Anal Calorim.* 2008;92: 887–92.
32. Frost RL, Wain D. A thermogravimetric and infrared emission spectroscopic study of alunite. *J Therm Anal Calorim.* 2008;91: 267–74.
33. Hales MC, Frost RL. Thermal analysis of smithsonite and hydrozincite. *J Therm Anal Calorim.* 2008;91:855–60.
34. Palmer SJ, Frost RL, Nguyen T. Thermal decomposition of hydrotalcite with molybdate and vanadate anions in the interlayer. *J Therm Anal Calorim.* 2008;92:879–86.
35. Vagvolgyi V, Daniel LM, Pinto C, Kristof J, Frost RL, Horvath E. Dynamic and controlled rate thermal analysis of attapulgite. *J Therm Anal Calorim.* 2008;92:589–94.
36. Vagvolgyi V, Frost RL, Hales M, Locke A, Kristof J, Horvath E. Controlled rate thermal analysis of hydromagnesite. *J Therm Anal Calorim.* 2008;92:893–7.
37. Vagvolgyi V, Hales M, Martens W, Kristof J, Horvath E, Frost RL. Dynamic and controlled rate thermal analysis of hydrozincite and smithsonite. *J Therm Anal Calorim.* 2008;92:911–6.
38. Zhao Y, Frost RL, Vagvolgyi V, Waclawik ER, Kristof J, Horvath E. XRD, TEM and thermal analysis of yttrium doped boehmite nanofibres and nanosheets. *J Therm Anal Calorim.* 2008;94:219–26.
39. Frost RL, Musumeci AW, Adebajo MO, Martens W. Using thermally activated hydrotalcite for the uptake of phosphate from aqueous media. *J Therm Anal Calorim.* 2007;89:95–9.
40. Palmer SJ, Frost RL. Characterisation of bauxite and seawater neutralised bauxite residue using XRD and vibrational spectroscopic techniques. *J Mater Sci.* 2009;44:55–63.
41. Palmer SJ, Frost RL, Nguyen T. Hydrotalcites and their role in coordination of anions in Bayer liquors: anion binding in layered double hydroxides. *Coord Chem Rev.* 2009;253:250–67.